An Enhanced Reduced Basis Method for Wideband Finite Element Method Simulations

DAMIAN SZYPULSKI[ID], **(Student Member, IEEE), GRZEGORZ FOTYGA**[ID], **(Member, IEEE),
AND MICHAL MROZOWSKI**[ID], **(Fellow, IEEE)**
Faculty of Electronics, Telecommunications, and Informatics, Gdańsk University of Technology, 80-233 Gdańsk, Poland
Corresponding author: Damian Szypulski (damian.szypulski@pg.edu.pl)

ABSTRACT In this paper, we present a novel strategy for selecting expansion points in the reduced basis method. A single computation of the error estimator is used to select a few expansion points in the multi-parameter space simultaneously. The number of selected points is determined adaptively, based on the accuracy of the current reduced model. The reliability and efficiency of this proposed approach are illustrated by numerical tests considering real-life structures, including dielectric resonator filter, H-plane filter, and four-pole dielectric-loaded cavity filter.

INDEX TERMS Model-order reduction, a posteriori error estimator, finite element method.

I. INTRODUCTION

Model-order reduction (MOR) techniques are commonly applied to expedite evaluations of the behavior of electromagnetic systems over wide frequency ranges. The main idea of MOR is to replace the original complex model with a much simpler approximated model that is accurate within a certain frequency band. In order to obtain reliable and compact reduced models for broadband frequency analysis, multipoint MOR methods must be applied. These assume that the projection basis is generated by solving a problem at a few carefully selected frequency points. In moment-matching techniques [1]–[6], frequency derivatives of the reduced and original transfer functions are matched up to the specified order at the selected expansion points. However, if the analyzed structure contains dispersive materials, the moment-matching techniques provide the reduced-order models (ROMs) which are valid only in a narrow frequency band.

In such cases, much more reliable are the so-called reduced-basis methods (RBM) [7], [8], which rely on the assumption that field solutions (snapshots) are collected from selected frequency points. The subsequent block moments or snapshots are used to form an orthogonal projection basis. What is important, RBM provides a much more compact basis, comparing to moment-matching based methods. Next, the Galerkin projection of the original full-order model is used to obtain a low-dimensional model. However, both multipoint approaches face the same challenge—how to chose expansion points that yield a reliable, compact ROM, while ensuring the efficiency of the reduction process.

A few approaches have been proposed to address this issue. A multipoint moment-matching method for fast high-speed VLSI interconnect analysis was used in [1]. Frequencies for expansion are chosen by a binary search algorithm that compares the values of two transfer functions at neighboring expansion points. In [2], the order of the reduced model and the placement of the subsequent expansion points are selected using criteria based on the convergence of a certain number of poles of the system. In [3], a multipoint moment-matching approach is presented in which the expansion points are chosen *a priori*. Reference [4] details the multipoint Galerkin asymptotic waveform evaluation, where the frequencies for ROM construction are selected based on the relative residual measure. Finally, in [9], a bisection point-placement strategy is considered.

There are also techniques [5]–[11] based on optimal greedy point selection algorithms. Subsequent expansion points are selected at frequencies where a residual-based *a posteriori* error estimator assumes its maximum. Moreover, error estimators are used to measuring the accuracy of the reduced model. The greedy multipoint MOR

technique [5], [6] makes use of the residual error associated with the computation of the scattering matrix and the error is verified only at the ports of the analyzed structure. A different strategy is considered in RBM approaches [8]–[10], where the error is evaluated over the whole frequency band by computing the Euclidean norm of the residual error. Finally, the RBM techniques proposed in [7], [11] rely on the dual norm of the residual. The error-estimator operates on low-dimensional matrices, so it can be evaluated fast. Notwithstanding this, when the analysis involves computing the scattering parameters over a wide frequency range, and when the final projection basis consists of many vectors, the error-estimator computational cost can be large. This cost can further increase when the FE simulation is used to compute the response of systems in multi-parameter space, where the parameters are associated with frequency, material properties and geometry of the analyzed structure [11]–[13].

In this paper, we propose a novel greedy strategy for selecting expansion points, which increases the efficiency of the standard RBM by reducing the estimation time. Unlike traditional techniques [5]–[11], in which the expansion points are selected one at a time, in the technique proposed here, a single computation of an error estimator in the whole multi-parameter space is used to pick few subsequent expansions simultaneously. In order to prevent the projection basis from becoming too large, the number of points selected in each iteration is different and depends on the accuracy of the current reduced model. The end result is an automated enhanced reduced-basis method (EnRBM), which is a cost-efficient alternative to the standard RBM.

II. BACKGROUND

Consider a second-order time-harmonic formulation of Maxwell's equations for the electric field E. We assume that the conductors can be lossy and their properties are described by a frequency-dependent surface impedance. Following the standard finite element method (FEM) procedure (see [14] for details), the problem to be solved reduces to a linear system:

$$(\mathbf{\Gamma} + s\gamma(s)\mathbf{G} + s^2\mathbf{C})\mathbf{E}(s) = s\mathbf{BI},$$
$$\mathbf{U} = \mathbf{B}^T\mathbf{E}(s). \quad (1)$$

where $\mathbf{\Gamma}$, $\mathbf{G}$, and $\mathbf{C}$ are $\mathbb{C}^{n \times n}$ system matrices, $\mathbf{E} \in \mathbb{C}^{n \times m}$ is the electric field solution matrix, $\mathbf{B} \in \mathbb{R}^{n \times m}$ is the normalized port selection matrix, m and n are the number of ports (assuming single-mode excitation) and the number of degrees of freedom (DoF), respectively, $\mathbf{I}$ is the normalized vector of amplitudes for modes at the ports, $\mathbf{U}$ - amplitudes of voltage waves, $s = j\omega/c = jk$ is the complex frequency, and finally $\gamma(s)$ is a scalar function modeling the dispersion of the surface impedance.

The number of unknowns (n) is often as high as a few million, and the analysis then becomes time consuming, especially when wide-band frequency analysis is needed. To speed up the frequency sweep, we consider the RBM method [7]–[11].

A. REDUCED BASIS METHOD

The RBM method relies on the observation that the electromagnetic field does not vary significantly inside a given frequency band of interest. The solution can thus be obtained in the reduced basis space spanned by N well-chosen solutions $\mathbf{E}(s_1), \mathbf{E}(s_2), \ldots, \mathbf{E}(s_N)$ computed at the expansion frequencies $s_1, s_2, \ldots, s_N$. To this end, the original system of equations is projected onto the reduced space:

$$\mathbf{Q} = span\{\mathbf{E}(s_1), \mathbf{E}(s_2), \ldots, \mathbf{E}(s_N)\}. \quad (2)$$

The orthogonality of the projection basis $\mathbf{Q}$ is ensured by the Gram–Schmidt process. Applying the Galerkin method with $\mathbf{Q}$ as basis and testing vectors, a reduced system is obtained:

$$(\mathbf{\Gamma}_r + s\gamma(s)\mathbf{G}_r + s^2\mathbf{C}_r)\mathbf{E}_r(s) = s\mathbf{B}_r\mathbf{I} \quad (3)$$

where the reduced matrices are given by: $\mathbf{\Gamma}_r = \mathbf{Q}^H\mathbf{\Gamma}\mathbf{Q} \in \mathbb{C}^{N \times N}$, $\mathbf{G}_r = \mathbf{Q}^H\mathbf{G}\mathbf{Q} \in \mathbb{C}^{N \times N}$, $\mathbf{C}_r = \mathbf{Q}^H\mathbf{C}\mathbf{Q} \in \mathbb{C}^{N \times N}$, $\mathbf{B}_r = \mathbf{Q}^H\mathbf{B} \in \mathbb{C}^{N \times m}$ and $\mathbf{E}(s) \approx \mathbf{Q}\mathbf{E}_r(s)$. The final number of degrees of freedom is much smaller, since $N \ll n$.

Each time a new solution matrix $\mathbf{E}(s_i)$ is appended to the projection basis $\mathbf{Q}$, the error introduced by the ROM is assessed by means of a correctly defined error estimator. The role of the estimator is twofold: Firstly, it is used as a stopping criterion—once the estimated error drops below a specified tolerance over the entire frequency band, the algorithm stops. Secondly, it guides the process of selecting expansion frequency points within the band of interest [f_{min}, f_{max}]. To this end, a greedy scheme is applied. That is, the next point is located at the frequency at which the estimated error is largest. It is worth mentioning that this kind of reduction scheme based on the error-estimator enables full automation of the reduction process, since at every stage of the reduction, we gain insight into the error introduced by the ROM.

In order to define the error estimator formula, we first have to formulate the residual error matrix. In [5], [8], an error estimator related to the residual of the scattering parameter FEM formulation was proposed:

$$\mathbf{R}(s) = 2s\mathbf{B} - (\mathbf{\Gamma} + s(\gamma(s)\mathbf{G} + \mathbf{B}\mathbf{B}^T) + s^2\mathbf{C})\mathbf{Q}\mathbf{E}_r(s) \quad (4)$$

where the reduced solution matrix $\mathbf{E}_r(s)$ is the solution of:

$$(\mathbf{\Gamma}_r + s(\gamma(s)\mathbf{G}_r + \mathbf{B}_r\mathbf{B}_r^T) + s^2\mathbf{C}_r)\mathbf{E}_r(s) = s\mathbf{B}_r\mathbf{I}. \quad (5)$$

Based on (4) and (5) we can efficiently assess the error introduced by the reduced order model using the following goal-oriented error estimator [5], [8]:

$$\begin{aligned}\mathbf{E}_s(s) = \mathbf{B}^T\mathbf{R}/|2s\mathbf{B}^T\mathbf{B}| = [2s\mathbf{B}^T\mathbf{B} - \mathbf{B}^T\mathbf{\Gamma}\mathbf{Q}\mathbf{E}_r \\ - s^2\mathbf{B}^T\mathbf{C}\mathbf{Q}\mathbf{E}_r - s\mathbf{B}^T\mathbf{B}\mathbf{B}^T\mathbf{Q}\mathbf{E}_r \\ - s\gamma(s)\mathbf{B}^T\mathbf{G}\mathbf{Q}\mathbf{E}_r]/|2s\mathbf{B}^T\mathbf{B}|. \quad (6)\end{aligned}$$

Note that the blocks of matrices $\mathbf{B}^T\mathbf{B}$, $\mathbf{B}^T\mathbf{\Gamma}\mathbf{Q}$, $\mathbf{B}^T\mathbf{C}\mathbf{Q}$, $\mathbf{B}^T\mathbf{B}\mathbf{B}^T\mathbf{Q}$ and $\mathbf{B}^T\mathbf{G}\mathbf{Q}$ are frequency-independent and can be computed only once, in the prepossessing stage, so-called *offline*. More precisely (following [7]), the offline stage comprises all the computations with complexity depending on n, which are performed only once. On the other hand, the *online*

phase concerns all the computations with the complexity depending on N, including error estimation process (6) and fast frequency sweep (5), which is used to compute the scattering parameters of the structure.

The above definition of the error estimator is used to fully control the reduction algorithm in terms of the stopping criteria, as well as the expansion point selection. Although the estimator operates on low-order matrices, it must be computed at each frequency within the band of interest, every time a projection basis is expanded. For wide-band simulations, this may significantly increase the numerical effort required for the reduction process. In order to improve the estimation efficiency, we propose a novel approach, called the enhanced reduced-basis method (EnRBM), in which a few expansion points are added simultaneously with each evaluation of the error estimator. To prevent the resulting basis from growing too large, the number of expansion points added at one time is chosen adaptively, based on the current value of the estimator.

B. ENHANCED RBM ALGORITHM (ENRBM)

The proposed EnRBM algorithm is summarized in the pseudocode in Algorithm 1 and Algorithm 2. It begins with specification of the input parameters: lower and upper frequency limits ($f_{\min}$, $f_{\max}$), the number of frequency points (n_f), the error tolerance (*tol*), the maximum number of points selected in a single iteration ($N_{\max}$), and the coefficient Δ_w—a positive number $\ll 1$ associated with the threshold level of the estimated error, below which candidates for additional expansion points are not taken into account. Finally, we define the minimal distance Δ_f between the chosen expansion points. We also need to specify the initial frequency expansion points. Standard approaches begin with

---

Algorithm 1 EnRBM: Enhanced RBM Procedure

Require: $f_{\min}, f_{\max}, n_f$, *tol*, $\mathbf{B}, \mathbf{C}, \mathbf{G}, \boldsymbol{\Gamma}$
1: Offline stage: compute components $\mathbf{B}^T\mathbf{B}$, $\mathbf{B}^T\mathbf{C}$, $\mathbf{B}^T\mathbf{G}$, $\mathbf{B}^T\boldsymbol{\Gamma}$
2: $\mathbf{f}_x = [f_{\min} \quad (f_{\min} + f_{\max})/2 \quad f_{\max}]$ // Initial expansion points
  $\Delta_w = 0.1 \quad \Delta_f = 0.05\,\text{GHz} \quad jj = 1$
3: **while** $e_{\max}^{\text{global}} > tol$ **do**
4:   SET $ii \leftarrow 1$
5:   **while** $ii \leq length(\mathbf{f}_x)$ **do**
6:     For given $s = j2\pi f_x(ii)$ compute:
  $\mathbf{A} = \boldsymbol{\Gamma} + s\gamma(s)\mathbf{G} + s^2\mathbf{C}, \quad \mathbf{Q}_{jj} = s\mathbf{A}^{-1}\mathbf{B}$
7:     $\mathbf{Q} = GS(\mathbf{Q}, \mathbf{Q}_{jj})$ Gram-Schmidt process
8:     $[\cdot] = \text{UPDATE}(\mathbf{C}_r, \boldsymbol{\Gamma}_r, \mathbf{G}_r, \mathbf{B}_r, \mathbf{B}^T\mathbf{B}\mathbf{B}^T\mathbf{Q}, \mathbf{B}^T\mathbf{C}\mathbf{Q}, \mathbf{B}^T\mathbf{G}\mathbf{Q}, \mathbf{B}^T\boldsymbol{\Gamma}\mathbf{Q}, \mathbf{Q}, \cdot)$ // Offline components update
9:     Set $ii \leftarrow ii + 1 \quad jj \leftarrow jj + 1$
10:   **end while**
11:   $[e_{\max}^{\text{global}}, \mathbf{f}_x, \cdot] = \text{EstError}(\cdot)$ // Estimate error
12: **end while**
13: **return** $e_{\max}^{\text{global}}, \mathbf{C}_r, \boldsymbol{\Gamma}_r, \mathbf{B}_r, \mathbf{G}_r$

Algorithm 2 EstError: Fast S-Parameter Error Estimator

Require: $n_f, N_{\max}, \mathbf{f}$, *tol*, $\Delta_w, \mathbf{C}_r, \boldsymbol{\Gamma}_r, \mathbf{G}_r, \mathbf{B}_r$,
  $\mathbf{B}^T\mathbf{B}\mathbf{Q}, \mathbf{B}^T\mathbf{C}\mathbf{Q}, \mathbf{B}^T\mathbf{G}\mathbf{Q}, \mathbf{B}^T\boldsymbol{\Gamma}\mathbf{Q}$
1: Compute $\mathbf{E}_s(s)$ using (6)
2: Find local maxima vector $\mathbf{e}_{\max}$ (considering Δ_f), corresponding frequency vector $\mathbf{f}_x$ and global maximum value $e_{\max}^{\text{global}}$
3: Compute $N_{\max}$ using (7)
4: Limit number of expansion points to $N_{\max}$
5: Reject expansion points with values below $\Delta_w e_{\max}^{\text{global}}$
6: **return** $e_{\max}^{\text{global}}$

---

only one expansion point, either located in the middle of the bandwidth ($(f_{\min} + f_{\max})/2$) [5], [9] or chosen randomly [7]. In EnRBM, we assume that, besides the middle point, two additional points are initially chosen from the end of the band: the solutions at these points are the least linearly dependent with respect to the solution evaluated at the midpoint. Next, at the three initial points, the original FEM system of equations (1) is solved and the solution matrices are appended to the projection basis $\mathbf{Q}$, which is afterwards orthogonalized using the Gram-Schmidt algorithm.

In the next step, the error estimator (6) is computed using frequency-independent reduced matrices (see Algorithm 2 for details). Based on the error estimator, we now have to define new expansion points that provide, on the one hand, a significant increase in the fidelity of the reduced model, but on the other hand, do not expand the basis too much. To this end, the local maxima of the estimated error are found, and among them a few new expansion points are selected, based on the following criteria:

1) If the two selected expansion points are located too close to each other, the projection basis $\mathbf{Q}$ will contain redundant components. In order to prevent such a situation, the distance between the two points is calculated. If the distance is smaller than Δ_f, only one point with a larger error is retained.

2) The maximum number of expansion points in a single iteration should not be greater than N_{max}, which is selected adaptively on the basis of the current maximum value of the estimated error:

$$N_{\max} = \lfloor \log_{10}(e_{\max}^{\text{global}}/tol) \rfloor + 1. \quad (7)$$

This ensures that, in the initial stage, the number of points selected is relatively large and that the value of the error decreases quickly across the whole frequency band. In the final step, fine tuning is performed and only one point is added at a time.

3) The error introduced by the reduced model should be suppressed evenly over the entire frequency bandwidth; the local maxima, which are significantly below the current global maximum value of the error estimator, are therefore not considered. To this end, we compare all maxima to the global maximum $e_{\max}^{\text{global}}$ and consider

only the local maxima with values not smaller than $\Delta_w e_{\max}^{\text{global}}$.

Once a set of new points has been selected in the current iteration, the system of equations (1) is constructed and solved for the new expansion points. The solutions are then appended to the projection basis $\mathbf{Q}$. This process is executed until the maximum value of the error estimator $e_{\max}^{\text{global}}$ drops below *tol*. The subsequent snapshots added to the projection basis $\mathbf{Q}$ need to be orthogonalized with the Gram-Schmidt approach. Otherwise, the loss of orthogonality of $\mathbf{Q}$ leads to an ill-conditioned system of equations (3) and, in effect, the error estimator begins to differ significantly from the actual error.
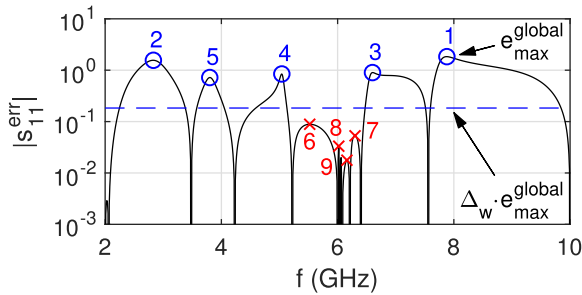

FIGURE 1. Expansion point selection.

Let us illustrate the above process with the simple example of the reduction for a bandwidth of 2–10 GHz with *tol* = $1e - 8$, as shown in Fig. 1. The error estimator has been computed and ten local maxima have been found, taking into account the minimum distance between the selected points ($\Delta_f = 0.05$ GHz). The global maximum value $e_{\max}^{\text{global}}$ is equal to 1.8, and so $N_{\max} = 9$ (computed using (7)). Thus only the first nine maxima are considered. Next, we reject the candidate points with error estimator values below the threshold, defined as $\Delta_w e_{\max}^{\text{global}}$, where $\Delta_w = 0.1$ (the threshold is denoted by the dashed horizontal line in Fig. 1, and the rejected candidates points 6–9 are indicated with crosses). Finally, the resultant set of expansion points, which will be used to generate new snapshots in the next iteration, consists of the first five local maxima, marked with the circles.

In effect, the proposed EnRBM approach selects a few expansion points simultaneously. It thus requires the error estimation to be computed significantly fewer times, than in the standard RBM approach. EnRBM is thus expected to result in substantial savings in the overall reduction time, especially when the bandwidth is large.

C. ENRBM FOR MULTI-PARAMETER FEM SYSTEMS

In the previous subsection, we have introduced the enhanced RBM approach for expedited solution of FE systems with a single parameter - frequency. However, the FEM-MOR technique can also be used for sweeps involving several parameters, associated not only with frequency but also with material properties and geometry of the structures [11]–[13]. EnRBM can be easily extended to multi-parameter systems,

provided the parameters are of the affine type. In the case of the non-affine parameter dependence, firstly the affine parameterization has to be extracted from the original system, using e.g. [13], [15], [16].

Here, for the sake of simplicity, we will consider FE systems with frequency and dielectric permittivity taken as parameters. More precisely, let us consider computational domain Ω divided into M non-overlapping subdomains:

$$\Omega = \bigcup_{m=1}^{M} \Omega_m, \tag{8}$$

where Ω_m contains a homogeneous, isotropic material, characterized by the frequency-independent relative permittivity $\varepsilon_{r,m}$. Hence, the vector of global parameters has the following form:

$$\mathbf{p} = [s, \varepsilon_{r,1}, \varepsilon_{r,2}, \ldots, \varepsilon_{r,M}] \in \mathbb{C}^{M+1}. \tag{9}$$

Taking into account the parameter-space, system (1) is transformed into:

$$(\mathbf{\Gamma} + s\gamma(s)\mathbf{G} + s^2 \sum_{m=1}^{M} (\varepsilon_{r,m}\mathbf{C}_m))\mathbf{E}(s) = s\mathbf{B}\mathbf{I},$$

$$\mathbf{U} = \mathbf{B}^T \mathbf{E}(s), \tag{10}$$

where the entries of the matrix associated with Ω_m subregion: $\mathbf{C}_m \in \mathbb{R}^{n \times n}$ are defined as follows:

$$c_{ij}^m = \int_{\Omega_m} (\vec{\alpha}_i \cdot \vec{\alpha}_j) d\Omega_m. \tag{11}$$

In the above formula, $\vec{\alpha}$ are the $H(curl)$ conforming FE basis functions. Similarly, equations (3) and (6) are transformed into:

$$(\mathbf{\Gamma}_r + s\gamma(s)\mathbf{G}_r + s^2 \sum_{m=1}^{M} (\varepsilon_{r,m}\mathbf{C}_{r,m}))\mathbf{E}_r(s) = s\mathbf{B}_r\mathbf{I} \tag{12}$$

and:

$$\mathbf{E}_s(s) = \mathbf{B}^T\mathbf{R}/|2s\mathbf{B}^T\mathbf{B}| = \left[2s\mathbf{B}^T\mathbf{B} - \mathbf{B}^T\mathbf{\Gamma}\mathbf{Q}\mathbf{E}_r\right.$$
$$- s^2 \sum_{m=1}^{M} \varepsilon_{r,m}\mathbf{B}^T\mathbf{C}_m\mathbf{Q}\mathbf{E}_r - s\mathbf{B}^T\mathbf{B}\mathbf{B}^T\mathbf{Q}\mathbf{E}_r$$
$$\left. - s\gamma(s)\mathbf{B}^T\mathbf{G}\mathbf{Q}\mathbf{E}_r\right]/|2s\mathbf{B}^T\mathbf{B}|. \tag{13}$$

Note that the response of the reduced-order model as well as the error indicator are computed in $M + 1$ dimensional space.

In order to apply the EnRBM approach in multi-variable space, only a few changes have to be considered, with regards to Algorithm 1 and Algorithm 2:

1) The initial expansion point is placed centrally in the parameter-space: $\mathbf{p}^c = [s^c, \varepsilon_{r,1}^c, \varepsilon_{r,2}^c, \ldots, \varepsilon_{r,M}^c]$.
2) The response of the reduced model, as well as the error indicator are computed using (12) and (13), respectively.
3) Additional reduced matrices have to be generated and stored: $\mathbf{C_m}$ and $\mathbf{B}^T\mathbf{C_m}\mathbf{Q}$, for $\mathbf{m} = 1 \ldots M$.

4) Let us assume that in a given iteration, n_G points have already been selected for expansion. The distance $\Delta \mathbf{p}^g$ between the next considered point and each of the already selected points should be greater than 1, assuming:

$$\Delta \mathbf{p}^g = \sqrt{\sum_{m=1}^{M+1} \left(\frac{2|p_m^p - p_m^{s,g}|}{(p_m^{max} - p_m^{min})} \right)^2} \quad \text{for } g = 1 \ldots n_G \tag{14}$$

where p_m^{max} and p_m^{min} are the maximum and minimum values of the p^m parameter, $p_m^{s,g}$ is the value of the m-th parameter of the already selected expansion point, and p_m^p is the value of the m-th parameter of the potential expansion point. Note that the equation (14) corresponds to the $(M+1)$-dimensional hyperellipsoid with the m-th semi-axes length equal to $(p_m^{max} - p_m^{min})/2$. Only the points which lie outside of the hyperellipsoid are selected.

D. LIMITATIONS OF ENRBM

The RBM-based simulations comprise the so-called *offline* and *online* steps (see Section IIA for details). Note that the proposed method affects only the online stage, which includes the error estimation process and the fast frequency sweep. Therefore, the overall speedup of simulations performed using EnRBM is high, only if the offline stage is not the dominating factor of computations. Hence, the proposed method is effective in the following cases:

1) The number of FEM variables is relatively small/medium so the system matrix factorization is not the dominating computational load. Such a situation occurs for example in the initial phases of the design process, which rely on the coarse (surrogate) models [17]. In such cases, the scattering characteristics of the coarse model have to be computed many times in different points of the parameters space. Hence, the overall simulation time can be large, although the number of FE unknowns is relatively small.

2) The number of frequency points, in which the scattering parameters are evaluated, is relatively large. Such simulation scenarios are considered for example if the goal of computations is to precisely extract the zeros and poles of a rational function, which approximates the scattering parameters [18] or when the simulation deals with the narrow-band structures, such as multiplexers or high-order filters.

3) The simulation deals with the multi-parameter space [12], [13]. In such cases, the error has to be estimated in many points of the parameter space, and thus the error estimation may become a bottleneck of the whole simulation.

III. NUMERICAL EXPERIMENTS

In this section, we use the proposed EnRBM approach on three structures: dielectric resonator filter, H-plane filter and

four-pole dielectric-loaded cavity filter. All simulations were carried out on a 64-bit workstation with a 3.00 GHz Intel i5-7400 processor and 32 GB of RAM in Matlab; however the Intel MKL PARDISO library was used for the solution of the original large system of FEM equations. Examples were prepared using InventSIM [20]. In all the tests, we assumed $\Delta_w = 0.1$.
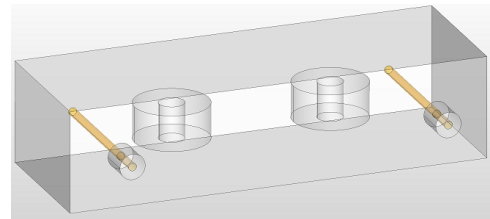
FIGURE 2. The geometry of dielectric resonator filter, dimensions are provided in [19].
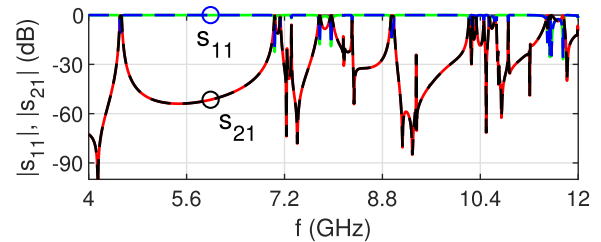
FIGURE 3. S parameters of dielectric resonator filter. Solid lines - reference, dashed lines - MOR.

In the first example, we considered a dielectric resonator filter, fed with an SMA connector, analyzed at 1801 points from 4 to 12 GHz. The structure is presented in Fig. 2 and the reference and MOR S-characteristics are shown in Fig. 3. The full FEM model consists of 101,264 variables, for which the direct frequency sweep took 1004.1 s.

Next, the filter has been analyzed by means of RBM and the proposed EnRBM, where we assumed $\Delta_f = 0.1$ and $tol = 1e-8$. The results can be seen in the Table 1. The number of vectors in the projection basis for both algorithms is the same (140), however the number of estimate computations is significantly higher (70 and 16, respectively). In effect, the online time is reduced from 41.8 s to just 11.0 s, whereas the overall simulation time is reduced from 97.5 s to 66.5 s.

TABLE 1. Analysis results, dielectric resonator filter, *tol* $= 1e-8$.

Algorithm	RBM	EnRBM
No. of estimates	70	16
Basis size	140	140
Total time (s)	97.5	66.5
Offline time (s)	54.9	54.8
Online time (s)	41.8	11.0
Fast sweep (s)	0.5	0.5
Approx. speedup	10.3	15.1
Est. max.	5.6e-09	4.2e-09
RAM memory	1.3 GB	1.3 GB

The accuracy of the reduced model in both cases is almost the same, whereas the speedup of computations is increased from 10.3 (RBM) to 15.1 (EnRBM).
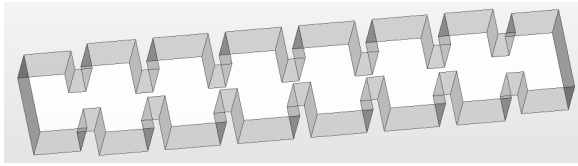

FIGURE 4. The geometry of H-Plane filter, dimensions are provided in [21].
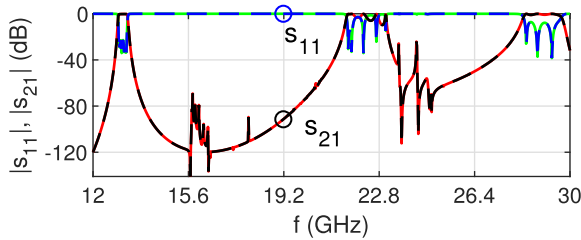

FIGURE 5. S parameters of H-Plane filter. Solid lines - reference, dashed lines - MOR.

The second numerical test deals with H-plane filter, considered at 1801 points from 12 to 30 GHz. The structure is presented in Fig. 4. The reference and MOR S-characteristics are shown in Fig. 5. We assumed that the structure exhibits frequency dependent conductor loss, namely that the conductivity of the walls is equal to $\sigma = 5.8e7$ S/m. The full FEM model consists of about 157,300 variables, for which the direct frequency sweep took 3124 s. Next, we analyzed the same structure using RBM and EnRBM, with $\Delta_f = 0.1$ and $tol = 1e - 6$. The number of vectors in the projection basis for both cases is the same (174), whereas the number of the error estimate computations is significantly higher (87 for RBM vs. 19 for EnRBM). In effect, the online time is reduced from 89.7 s to 20.5 s and the simulation time: from 325.8 s to 256.1 s. The accuracy of the reduced model is almost the same in both cases (1.5e-7 for RBM and 3.2e-7 for EnRBM), though the speedup increases from 9.6 to 12.2.

In the next numerical test, we have studied the efficiency of the proposed algorithm as a function of the number of frequency points (n_f). To this end, we have simulated the two considered structures for n_f varied from 201 to 1801. The results are shown in Fig. 6, and it can be seen that EnRBM considerably decreases the computational load of the online phase for all considered cases, whereas the memory consumption between RBM and EnRBM in both studied cases is negligible (see Tab 1-2 for details). The comparisons between the actual and estimated errors are shown in Fig. 7, where the actual error is defined as:

$$\mathbf{S}^{error}_{actual}(s) = \max|S(s)^{MOR} - S(s)^{REF}|, \qquad (15)$$

where S^{MOR} and S^{REF} are the scattering parameters of the structure, obtained by means of the reduced and the original

TABLE 2. Analysis results, H-plane filter, tol = 1e-6.

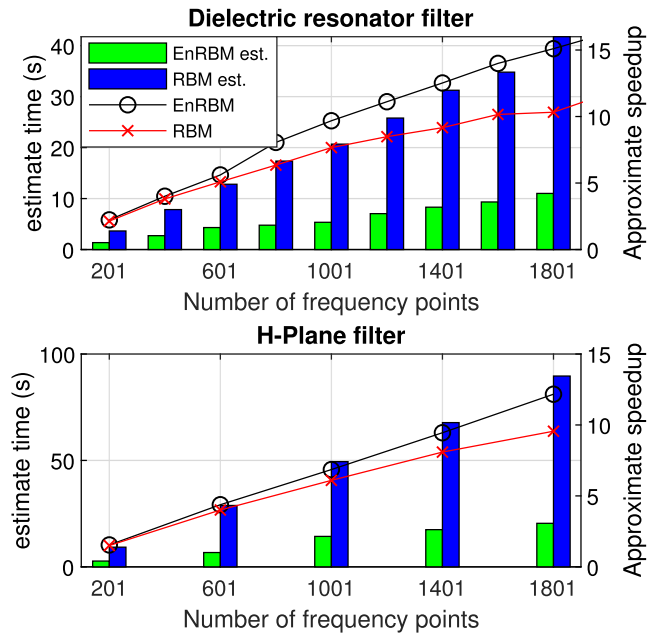| Algorithm	RBM	EnRBM
No. of estimates	87	19
Basis size	174	174
Total time (s)	325.8	256.1
Offline time (s)	233.5	233.4
Online time (s)	89.7	20.5
Fast sweep (s)	1.9	1.9
Approx. speedup	9.6	12.2
Est. max.	1.5e-07	3.2e-07
RAM memory	2.22 GB	2.22 GB

FIGURE 6. Online phase computational time as a function of the number of frequency points for RBM and EnRBM.

full-order FEM model, respectively. It can be seen that both error measures are well correlated and fall below the specified *tol.* level.

In the last numerical test we considered a four-pole dielectric-loaded cavity filter (Fig. 8), analyzed in the multivariable space. More precisely, the response of the system is a function of three parameters: frequency $p_1 = f = 11 \dots 12$ GHz, and relative permittivity of the pucks: $p_2 = \varepsilon_{r,1} = 26 \dots 34$ and $p_3 = \varepsilon_{r,2} = 26 \dots 34$, where the number of equidistantly distributed sampling points is 201, 19 and 9, respectively. The full FEM model consists of 130,238 variables, for which the direct sweep with respect to all three parameters (i.e. computations at 34731 points in a three dimensional space) took ≈ 21960 s. Figs. 9 and 10 show parametric plots of s_{11} and s_{12} where the value of $\varepsilon_{r,2}$ is fixed at 30.

Next, the structure has been analyzed using RBM and the proposed EnRBM methods. In both cases, the initial expansion point was placed centrally in the parameter space: $\mathbf{p}^C = [11.5, 30, 30]$. The subsequent expansion points have been selected following the error indicator (13), which
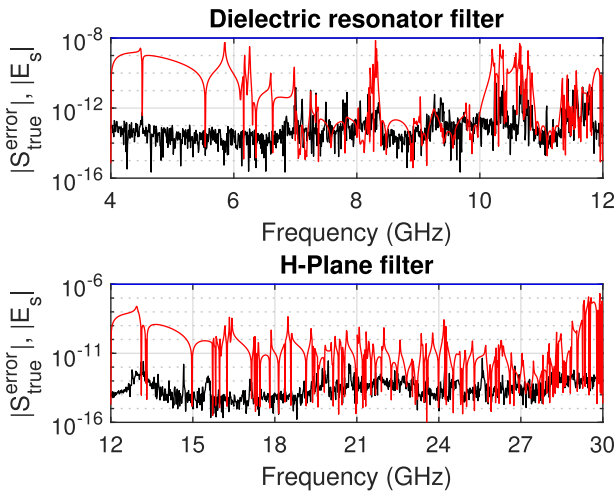
FIGURE 7. Comparison of actual error (black) and estimated (red) errors for the first two considered cases. The blue line specifies the tolerance level.
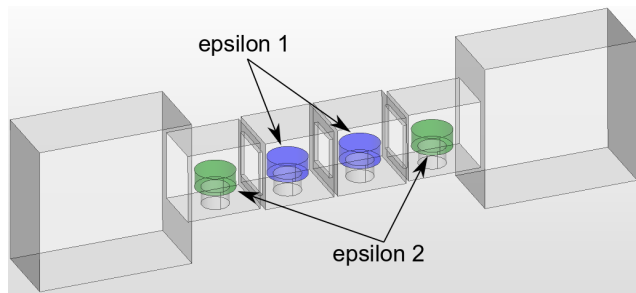

FIGURE 8. The geometry of the four-pole dielectric-loaded cavity filter, dimensions are provided in [22].
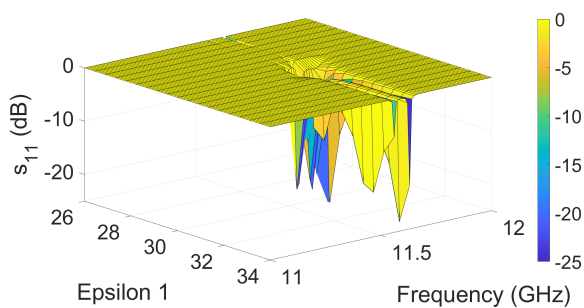

FIGURE 9. The S_{11} parameter-plot, where the $\varepsilon_{r,2}$ value is fixed at 30.

TABLE 3. Analysis results, dielectric-loaded cavity filter, *tol* $= 1e - 6$.

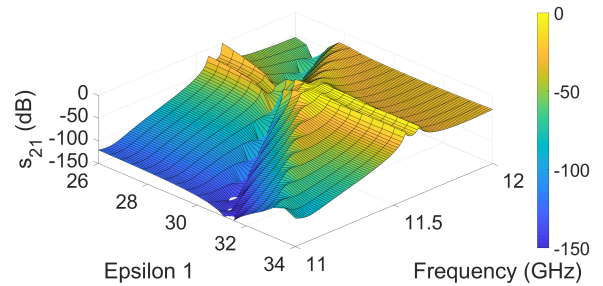| Algorithm	RBM	EnRBM
No. of estimates	71	27
Basis size	150	146
Total time (s)	975.1	444.3
Offline time (s)	91.0	88.1
Online time (s)	884.1	356.1
Pick Time (s)	0.0	0.1
Fast sweep (s)	13.7	13.0
Approx. speedup	22.6	49.7
Est. max.	6.6e-07	5.4e-07
RAM memory	2.11 GB	2.11 GB

FIGURE 10. The S_{21} parameter-plot, where the $\varepsilon_{r,2}$ value is fixed at 30.
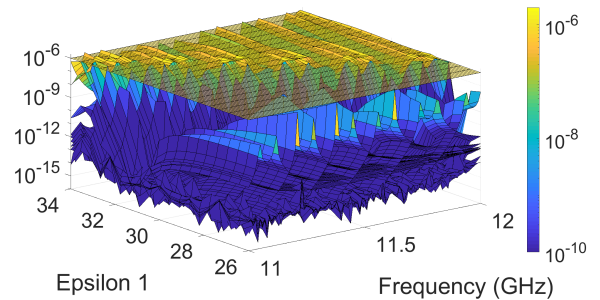

FIGURE 11. A four-pole dielectric-loaded cavity filter. The actual error as a function of $\varepsilon_{r,1}$ and frequency, for $\varepsilon_{r,2} = 26, 27, \ldots, 34$.

$\varepsilon_{r,2} = 26, 27, \ldots, 34$ is presented in the Fig. 11. It can be seen that in the whole parameter-space, the actual error is below *tol* (1e-6), indicated by the yellow transparent plane.

IV. CONCLUSIONS

In this paper, a systematic process has been presented for enhancing the efficiency of the Reduced Basis Method. In contrast to the standard RBM approach, a few expansion points in the multi-parameter space are selected with a single computation of the error estimator. The number of expansion points is determined adaptively based on the accuracy of a current reduced model. Numerical examples show that this proposed technique substantially improves the efficiency of the reduced-basis approach, without affecting the size of the projection basis.

REFERENCES

[1] R. Sanaie, E. Chiprout, M. S. Nakhla, and Q. J. Zhang, "A fast method for frequency and time domain simulation of high-speed VLSI interconnects," *IEEE Trans. Microw. Theory Techn.*, vol. 42, no. 12, pp. 2562–2571, Dec. 1994.

operated in the whole parameter-space. Table 3 compares the results of the simulations performed by means of RBM and EnRBM. It can be seen that unlike in previous examples, the online time is dominant, however this is more than two times shorter in the EnRBM comparing to RBM. As discussed in Section II.D, EnRBM is expected to outperform RBM exactly in such situation. Indeed by using EnRBM instead of RBM, the overall speedup of simulations increases from 22.6 to 49.7, whereas the estimated error is almost at the same level ($6.6e − 07$ and $5.4e − 07$, respectively). The actual error as a function of $\varepsilon_{r,1}$ and frequency, for

[2] E. Chiprout and M. S. Nakhla, "Analysis of interconnect networks using complex frequency hopping (CFH)," *IEEE Trans. Comput.-Aided Design Integr. Circuits Syst.*, vol. 14, no. 2, pp. 186–200, Feb. 1995.

[3] T. V. Narayanan and M. Swaminathan, "Preconditioned second-order multi-point passive model reduction for electromagnetic simulations," *IEEE Trans. Microw. Theory Techn.*, vol. 58, no. 11, pp. 2856–2866, Nov. 2010.

[4] R. D. Slone, J.-F. Lee, and R. Lee, "Automating multipoint Galerkin AWE for a FEM fast frequency sweep," *IEEE Trans. Magn.*, vol. 38, no. 2, pp. 637–640, Mar. 2002.

[5] M. Rewienski, A. Lamecki, and M. Mrozowski, "Greedy multipoint model-order reduction technique for fast computation of scattering parameters of electromagnetic systems," *IEEE Trans. Microw. Theory Techn.*, vol. 64, no. 6, pp. 1681–1693, Jun. 2016.

[6] G. Fotyga, M. Czarniewska, A. Lamecki, and M. Mrozowski, "Reliable greedy multipoint model-order reduction techniques for finite-element analysis," *IEEE Antennas Wireless Propag. Lett.*, vol. 17, no. 5, pp. 821–824, May 2018.

[7] V. de La Rubia, U. Razafison, and Y. Maday, "Reliable fast frequency sweep for microwave devices via the reduced-basis method," *IEEE Trans. Microw. Theory Techn.*, vol. 57, no. 12, pp. 2923–2937, Dec. 2009.

[8] M. Rewienski, A. Lamecki, and M. Mrozowski, "A goal-oriented error estimator for reduced basis method modeling of microwave devices," *IEEE Microw. Wireless Compon. Lett.*, vol. 25, no. 4, pp. 208–210, Apr. 2015.

[9] Y. Konkel, O. Farle, A. Köhler, A. Schultschik, and R. Dyczij-Edlinger, "Adaptive strategies for fast frequency sweeps," *COMPEL-The Int. J. Comput. Math. Elect. Electron. Eng.*, vol. 30, no. 6, pp. 1855–1869, Nov. 2011.

[10] V. de La Rubia, "Reliable reduced-order model for fast frequency sweep in microwave circuits," *Electromagnetics*, vol. 34, nos. 3–4, pp. 161–170, 2014.

[11] M. W. Hess and P. Benner, "Fast evaluation of time–harmonic Maxwell's equations using the reduced basis method," *IEEE Trans. Microw. Theory Techn.*, vol. 61, no. 6, pp. 2265–2274, Jun. 2013.

[12] S. Burgard, O. Farle, and R. Dyczij-Edlinger, "An adaptive sub-domain framework for parametric order reduction," *IEEE Trans. Magn.*, vol. 51, no. 3, Mar. 2015, Art. no. 7208504.

[13] M. K. Sampath, A. Dounavis, and R. Khazaka, "Parameterized model order reduction techniques for FEM based full wave analysis," *IEEE Trans. Adv. Packag.*, vol. 32, no. 1, pp. 2–12, Feb. 2009.

[14] M. Rewieński, A. Lamecki, and M. Mrozowski, "Model order reduction for problems with dispersive surface boundary conditions," *IEEE Microw. Wireless Compon. Lett.*, vol. 25, no. 9, pp. 561–563, Sep. 2015.

[15] S. Burgard, O. Farle, and R. Dyczij-Edlinger, "A novel parametric model order reduction approach with applications to geometrically parameterized microwave devices," *COMPEL-Int. J. Comput. Math. Elect. Electron. Eng.*, vol. 32, no. 5, pp. 1525–1538, 2013.

[16] M. A. Grepl, Y. Maday, N. C. Nguyen, and A. T. Patera, "Efficient reduced-basis treatment of nonaffine and nonlinear partial differential equations," *ESAIM, Math. Model. Numer. Anal.*, vol. 41, no. 3, pp. 575–605, May 2007.

[17] J. W. Bandler, Q. S. Cheng, N. K. Nikolova, and M. A. Ismail, "Implicit space mapping optimization exploiting preassigned parameters," *IEEE Trans. Microw. Theory Techn.*, vol. 52, no. 1, pp. 378–385, Jan. 2004.

[18] N. Leszczynska, L. Szydlowski, and M. Mrozowski, "Zero-pole space mapping for CAD of filters," *IEEE Microw. Wireless Compon. Lett.*, vol. 24, no. 9, pp. 581–583, Sep. 2014.

[19] J. R. Brauer and G. C. Lizalek, "Microwave filter analysis using a new 3-D finite-element modal frequency method," *IEEE Trans. Microw. Theory Techn.*, vol. 45, no. 5, pp. 810–818, May 1997.

[20] A. Lamecki, L. Balewski, and M. Mrozowski, "An efficient framework for fast computer aided design of microwave circuits based on the higher-order 3D finite-element method," *Radioengineering*, vol. 23, no. 4, pp. 970–978, 2014.

[21] J. A. Ruiz-Cruz, J. R. Montejo-Garai, and J. M. Rebollar, "Computer aided design of waveguide devices by mode-matching methods," in *Passive Microwave Components and Antennas*. Rijeka, Croatia: InTech, 2010.

[22] F. Alessandri *et al.*, "The electric-field integral-equation method for the analysis and design of a class of rectangular cavity filters loaded by dielectric and metallic cylindrical pucks," *IEEE Trans. Microw. Theory Techn.*, vol. 52, no. 8, pp. 1790–1797, Aug. 2004.

DAMIAN SZYPULSKI (S'19) received the M.S.E.E. degree in microwave engineering from the Gdańsk University of Technology, Gdańsk, Poland, in 2018, where he is currently pursuing the Ph.D. degree with the Department of Microwave and Antenna Engineering. His current research interest includes computational electromagnetics, mainly focused on the finite-element method and model-order reduction techniques for the analysis of microwave devices.

GRZEGORZ FOTYGA (M'19) received the M.S.E.E. and Ph.D. degrees in electronic engineering from the Gdańsk University of Technology, in 2009 and 2016, where he is currently an Assistant Professor with the Department of Microwave and Antenna Engineering. His current research interests include computational electromagnetics, numerical methods, the finite element method, and model order reduction.

MICHAL MROZOWSKI (S'88–M'90–SM'02–F'08) received the M.Sc. and Ph.D. degrees (Hons.) from the Gdańsk University of Technology, in 1983 and 1990, respectively. He joined the Faculty of Electronics, Gdańsk University of Technology, in 1986, where he is currently a Full Professor, the Head of the Department of Microwave and Antenna Engineering, and the Director of the Center of Excellence for Wireless Communication Engineering. His current research interests include computational electromagnetics, GPU computing, the CAD of microwave devices, filter design, and optimization techniques.

● ● ●